JACS
JOURNAL OF THE AMERICAN CHEMICAL SOCIETY

Communication

pubs.acs.org/JACS

Ultralong Polarization Chains Induced by Ions Solvated in Confined Water Monolayers

Ishai Strauss,[†] Henry Chan,[†] and Petr Král*[,†,‡]

[†]Department of Chemistry and [‡]Department of Physics, University of Illinois at Chicago, Chicago, Illinois 60607, United States

ABSTRACT: We disclose by classical molecular dynamics simulations the formation of long polarization chains induced by ions solvated in a water monolayer confined between graphene sheets. First, we examine the dynamics of confined pure water clusters with $N_w < 100$ at temperatures of 200−300 K. We show that for certain "magic" N_w the clusters form crystallites with stable structures, where discrete water rings are self-organized with clockwise or anticlockwise orientations of their dipoles. Next, we show that when ions are hydrated in larger clusters with a "bracketed" crystal structure, they can generate long fluctuating chains of ($N_w > 30$) polarized waters. The chains generated by opposite charged ions can eventually meet, lock, and stay polarized at room temperatures.

Water confined in low dimensions has properties different from bulk water, which is essential for functioning of biological systems.[1,2] Water intercalated in narrow carbon nanotubes forms cylindrical monolayers of different thermodynamic and transport properties.[3−7] Surface tension in water nanodroplets placed on graphene-based nanostructures may induce their self-assembly.[8] Water droplets locked between graphene layers can form reaction nanocontainers.[9,10] Water confined between more rigid graphite layers or adsorbed at various surfaces can form quasi-2D crystals stable at room temperatures.[11−14] While progress on how inert gases solvate in confined environments has been made,[15] it is not clear how ions solvate in confined water layer and influence its structure.

Here, we study by classical molecular dynamics (MD) simulations the structure of water with solvated ions trapped between two graphene sheets. The systems are described by NAMD[16,17] and the CHARMM27 force field.[18] The (nonbonding) van der Waals (vdW) coupling between different atoms is described by a Lennard-Jones potential with the parameters for TIP3 water and carbon atoms, $\epsilon_C = -0.07$ kcal/mol, $R_{min,C} = 3.98$ Å. We use the Langevin dynamics with a damping coefficient[19,20] of 0.01 ps^{-1} and a time step of 2 fs. The systems are simulated in the NVT ensemble using the PME method for long-range electrostatics.[21]

First, we simulate pure water confined between two graphene sheets. We prepare two flat (9×9 nm^2) graphene sheets and place a water droplet ($N_w = 170$) between them. We minimize the system and then fix a few rows of atoms at the graphene edges (at a vdW distance of ∼3 Å from each other) to prevent water from escaping (if the edges are not fixed water is expelled at high speed). After equilibration for 10 ns, the water droplet forms a monolayer crystal with a "bracketed" crystal structure of C4 symmetry. In the area where a water monolayer is stabilized between the graphene sheets, the interlayer distance is ∼7 Å.

In Figure 1 (top left and middle), we show the top and side views of a larger 2D crystal (2048 water molecules) with the same crystal structure preassembled between two graphene layers (17×17 nm^2) and equilibrated for 1 ns at $T = 250$ K. In Figure 1 (top right), we show detail of the 2D water crystal between the graphene sheets. The crystal structure is preserved at room temperatures (our simulations show that the confined water crystals melt at $T_{melt} \sim 325$ K). Such crystal structure was

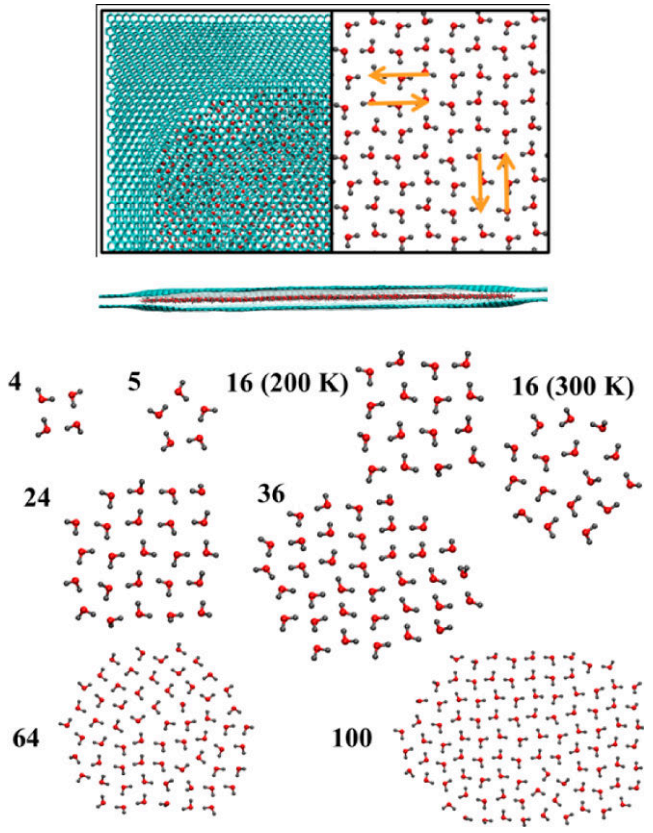


Figure 1. (top left) One quarter of a system of 2048 water molecules sandwiched between two graphene sheets (17×17 nm^2). (top right) Bracketed structure of 2D water crystal. Consecutive chains with alternating net dipole directions are emphasized. (middle) Side view of the graphene-water cell. (bottom) Small, equilibrated, planar water clusters confined between two relaxed graphene layers.

Received: August 29, 2013
Published: January 7, 2014

 © 2014 American Chemical Society dx.doi.org/10.1021/ja4087962 | J. Am. Chem. Soc. 2014, 136, 1170−1173

also observed to form at room temperature when water was confined between rigid graphitic slabs.[14]

The observed bracketed structure of water molecules is a result of the highly confined environment caused by the two graphene layers and the tendency of water molecules in a monolayer to maximize the number of hydrogen bonds (4). In a multilayer of ice on graphene, water molecules in the first ice layer are arranged hexagonally to position their oxygen atoms in the center of the carbon rings, but they are not completely parallel with the graphene plane.[22,23] It is of interest to find how the bracketed water structure is modified in small water clusters and in the presence of solutes.

We also briefly simulate small planar clusters of pure water[24,25] ($N_w < 100$) confined between two graphene layers (9 × 9 nm^2). The clusters are equilibrated in the same manner as before for several ns at $T = 200$ K. Smaller clusters ($N_w < 37$) gain stable structures within several ps, while larger ones equilibrate slower. After the equilibration, we find that clusters with certain "magic numbers"[26] ($N_w = 4, 5, 16, 24$) reach stable structures, which might depend on temperature.

In Figure 1 (bottom) we show several equilibrated planar water clusters. Small clusters ($N_w < 25$) acquire highly stable structures with water dipoles[27] arranged in concentric rings, in analogy to dipolar particles.[28] The $N_w = 4, 5$ clusters form a single ring of dipoles. The $N_w = 16$ clusters form two-ring structures of n/m waters in the first/second rings. The squarish (4/12) structure (a piece of the bracketed lattice) with opposite arrangement of dipoles in the two rings is stable at $T \approx 200$ K. The circular (5/11) arrangement with dipoles oriented in the same way in both rings is relatively stable at $T = 250–300$ K (frequently switches between transient states). The cluster with $N_w = 24$ whose inner two rings are of the same geometry as $N_w = 16$ (200 K structure) is also stable at $T \approx 200$ K. The $N_w = 36$ cluster tends to organize at $T = 200$ K into a structure with two large antiparallel dipoles. As the planar clusters become larger they tend to gain the crystalline form shown in Figure 1 (top right).

Next, we introduce one Na^+ or Cl^- ion in the center of the water ($N_w = 2048$) cluster in Figure 1 (top) to see how it perturbs the bracketed crystal structure. We equilibrate the whole system for $t = 10$ ns at $T = 300$ K. As seen in Figure 2 (bottom), the Na^+ ion polarizes four water molecules within its first hydration shell. Surprisingly, it turns out that the solvated ion can also transiently polarize[29] waters in the form of long chains of varying lengths, extending along four directions of the bracketed crystal structure, as shown in Figure 2 (bottom). During the chain formation, first a water that is the nearest to the ion flips its orientation. Then, this water flipping propagates, until the chain reaches a certain length (observed up to 30 waters). Eventually the chain collapses in the opposite sequence of events, and new chains form.

Within the ion-polarized chain, each of the water molecules flips the position of one of its hydrogen atoms in the direction outward from (Na^+) or inward to (Cl^-) the ion. Since a perfect crystal is formed by parallel chains[30,31] of water molecules with alternating dipole directions, as seen in Figure 1 (top right), when the ion flips the orientations of waters in a single chain, water dipoles in three neighboring chains gain the same orientations. In Figure 2 (bottom), these three chains with parallel water dipoles are seen to run through (orthogonal to) a visualized stripe of dipoles.

We can describe the induced water chains by a classical canonical ensemble with the configuration probabilities, $p_i = e^{-E_i/(k_BT)}/Z$ (partition function: $Z = \Sigma_i p_i$), where E_i are the chain configuration (microstate) energies (averaged over the rest of the system). Here, we calculate these configuration energies as follows: First, we prepare a perfect water crystal (50 × 50 nm^2), equilibrate it for 1 ns at 300 K, and insert a Na^+ ion in its center. Then, we sample the system in 500 fs intervals over 2.5 ns to track the chains of different lengths formed in the four possible directions from the ion. The probability, p_i, of observing a water chain with i waters is proportional to its existence time, t_i. Therefore, we can obtain the relative probabilities of neighboring chain configurations (lengths of $i/i-1$ waters) by measuring the relative existence times

$$c_i = \frac{p_i}{p_{i-1}} = \frac{t_i}{t_{i-1}} = e^{-\Delta E_i/(k_BT)} \quad (2)$$

where $\Delta E_i = E_i - E_{i-1}$ are the flipping energies between neighboring chain configurations. The configuration energies can be obtained by summing the flipping rates

$$E_i = E_0 - k_BT \sum_{i}^{j=1} \ln c_j \quad (3)$$

In Figure 2 (top), we show the flipping and configuration energies, ΔE_i ($E_0 = 0$) and E_i, respectively. We can see that the flipping energies are relatively small ($\Delta E_i \approx 0.1$ kcal/mol), but they gradually increase with the distance from the ion (polarization becomes more difficult away from the charge

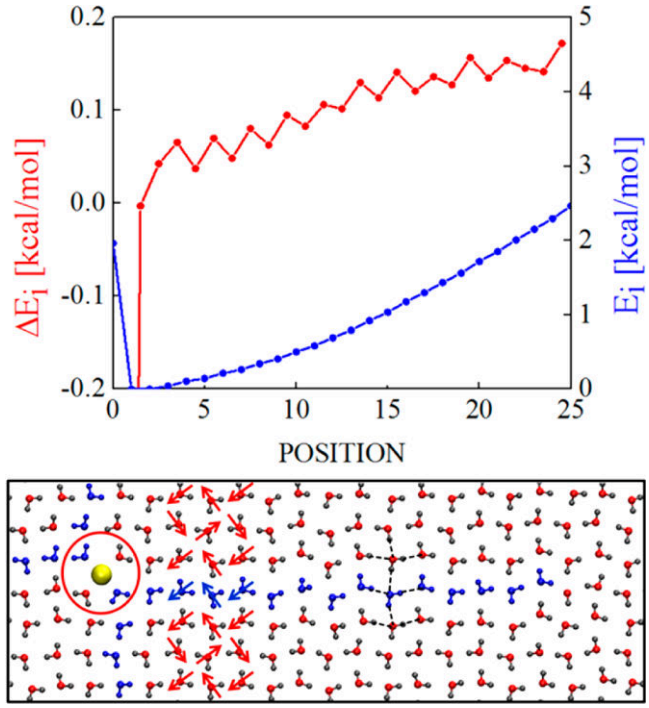


Figure 2. (top) Configuration and flipping energies of a water cluster with a bracketed structure and Na^+ ion in its center are shown as functions of the water flip position. The flipping energy for the first flip is largely negative (solvation shell formation). (bottom) A chain with 15 flipped water molecules extended from the solvated Na^+ ion. The water polarization starts at the ion hydration shell (circled) and proceeds in four orthogonal directions (emphasized). Water dipoles are visualized in a stripe orthogonal to the polarization chain. Hydrogen bonds are emphasized by dashed black lines. Upon flipping the water molecules maintain the same number (4) of hydrogen bonds.

dx.doi.org/10.1021/ja4087962 | J. Am. Chem. Soc. 2014, 136, 1170–1173

source). This leads to a weak nonlinear dependence of the chain configuration energies E_i on the position i.

The ions naturally induce a particular orientation around them, which is incompatible with the orientation of the bracketed structure. However, the flipping of the water molecules in the lines where the perturbation occurs produces a configuration (with the polarization lines) compatible with the tendency to maximize hydrogen bonds (the square-like bonded structure is maintained). The low energetic cost of flipping water molecules is associated with the fact that the flipping process practically does not change the number of hydrogen bonds. This is true even when the hydrogen of the flipping water molecule is pointing up (Figure 2 bottom).

Next, we briefly investigate the average chain length, $\langle L_i \rangle$, in dependence on temperature. We set the crystallite area to $S \approx 2{,}500$ nm^2, simulate the ion-crystal system as before and average the results over a 1 ns trajectory. We observe chains with an average length of $\langle L_i \rangle \approx 8.61$, 7.34, and 7.09 waters at a temperatures of $T = 300$, 200, and 100 K, respectively. We can compare these values with the average chain lengths obtained from the above model. The average chain lengths calculated using the E_i energies extracted as explained above are $\langle L_i \rangle = \sum_i L_i p_i \approx 6.85$, 5.50, and 3.79 waters at $T = 300$, 200, and 100 K, respectively. These values are close to the observed simulation lengths, especially at $T = 300$ K when the flipping energies (averaged over the other degrees of freedom) were obtained. The more frequent formation of longer polarized chains at higher temperature can result from increased thermal (defect nucleation) energy. Since the formation of polarized chains deforms the energetically more stable bracketed structure, the extra thermal energy is needed for the deformation (chain formation) to occur more often.

We also examine if the size of the 2D water crystallite affects the chain formation ability. At $T = 300$ K, we observe the average chain lengths of $\langle L_i \rangle \approx 11.54$, 11.48, and 8.91 waters for roughly circular crystals with areas of $S \approx 900$, 1600, and 2500 nm^2, respectively. The increasing chain length observed in smaller circular crystallites could be due to the surface tension effect of the crystallite edges. Surface tension tends to minimize the crystallite circumference and leads to round crystallites. However, the C4 symmetry of the bracketed structure prefers the formation of squarish crystallites. Since small crystallites have a higher edge to area ratio (stronger edge effect), the bracketed structure in these crystallites is less stable. Therefore, the ion in the center of the crystal can more easily disrupt the stable bracketed structure and flip the water molecules.

We also investigate water chains formed around (opposite) ion pairs. We prepare a 2D crystal of 2048 water molecules confined between the above graphene sheets (17×17 nm^2) and then relaxed at $T = 200$ K for $t = 1$ ns. In this crystal, we place one Na^+ and one Cl^- ions on the same crystal diagonal (direction of chain formation) and separate them by 18 waters. Then, we equilibrate the system for $t = 10$ ns at $T = 300$ K. As shown in Figure 3 (top), the two ions form a water chain[32] (bridge) connecting them. This chain is stable, and it does not fluctuate like chains formed around individual ions. When larger systems (≈33 000 water molecules) are simulated at $T = 300$ K, we observe that this water bridge can be highly stable even at large ion separations (up to 55 water molecules).

From these observations, we might conclude that larger oppositely charged regions could also communicate via water polarization. To follow this idea, we study how oppositely charged "electrodes" represented by small graphene regions

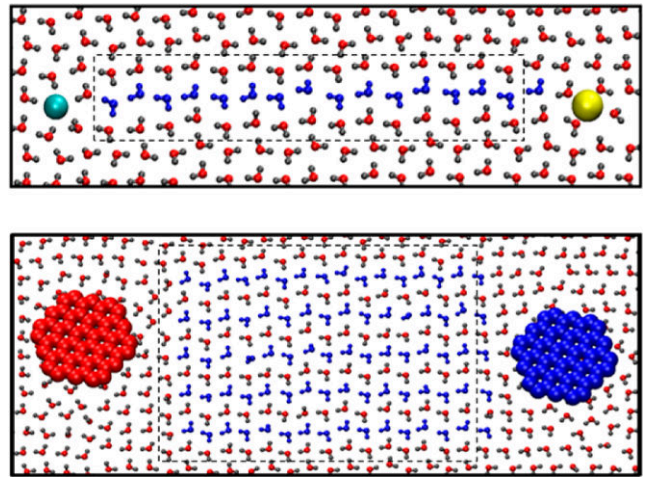


Figure 3. (top) A stable polarization bridge formed between Na^+ and Cl^- ions. (bottom) A wide polarization stripe stretched between two "electrodes" charged by ±5 e.

interact through the water layer. We select two circular regions in the upper graphene layer, each formed by 54 atoms, and oppositely charge them with |5e|, as seen in Figure 3 (bottom). The electrodes are arranged in line with the naturally occurring water chains, and their centers are separated by ≈5.3 nm. The systems are simulated as before at $T = 300$ K.

Figure 3 (bottom) illustrates that the induced water polarization in this two-electrode system is analogous to the two-ion system, but on a more massive scale. We observe that 5 water chains flip their orientations, seemingly in response to 5 times larger charge on each electrode. This leads to the formation of 11 parallel water chains with the same orientation of their dipoles. This wide polarized stripe provides large connectivity between the charged regions, which can be used in a potential communication between them.

We can envision that the graphene systems having a confined water monolayer could be prepared as shown in Figure 4 (brief simulations performed at 200 K). First, several graphene layers are positioned on a rigid substrate (e.g., metal) to maintain their flatness (first graphene layer is fixed). In the last graphene layer a ∼5 nm wide elongated window is made with hydrogen-terminated carbons. In this window, a small water droplet ($N_w \sim 1000$) with a hydrated Na^+ ion is deposited. Then, the system is closed by a multilayer (for additional rigidity) graphene. In the simulations, the top graphene layers are forced to move down until they are separated from the bottom layers by ∼3.4 Å. Then, the squeezing force is removed entirely, and the structure is briefly relaxed. Eventually, the top graphene layers seal a water monolayer underneath by vdW coupling to the bottom layers. Upon further equilibration the water should crystallize more, and ion-induced polarization chains should emerge. These polarization phenomena could be observed through the graphene layers by optical or electronic detection techniques.

In summary, we have used classical MD simulations to study planar water−ion structures confined between graphene monolayers. We observed stabilization of small pure water crystallites with a discrete number of rings of dipoles organized in a cocircular or counter-circular manner. When ions are hydrated in the 2D water monolayers they "shoot" long polarized water chains. The chains from opposite ions (electrodes) eventually meet, lock, and remain polarized.

dx.doi.org/10.1021/ja4087962 | J. Am. Chem. Soc. 2014, 136, 1170−1173

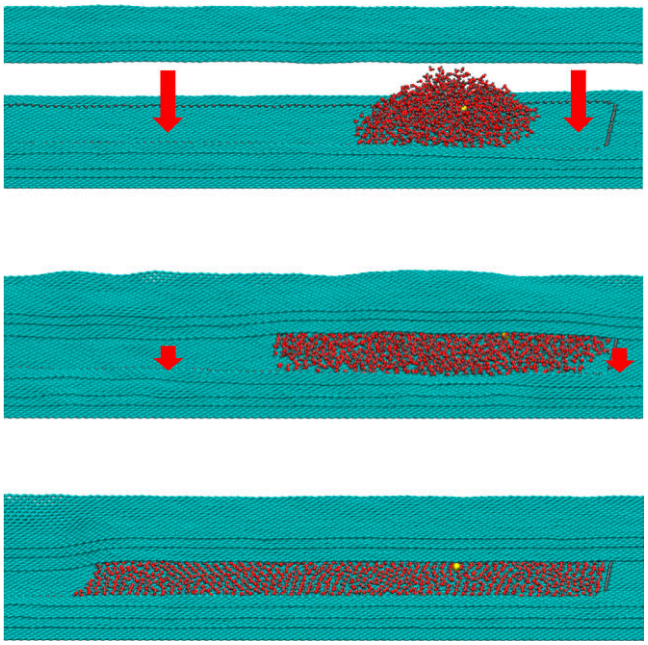


Figure 4. Simulated experimental setup. (top) A droplet with $N_w \sim 1000$ is placed in a ~5 nm wide hydrogenated window formed in the graphene monolayer (top layers are cut in half for clarity of view). Bottom layer is fixed, and top layers are moved down. (middle) The upper graphene layers are lowered by force until they are ~3.4 Å from the bottom layers. (bottom) The top layers are relaxed in the absence of a squeezing force (their distance is adjusted by the vdW attraction), and the confined water monolayer starts to crystallize.

These phenomena might be used in communication and information storage.

AUTHOR INFORMATION

Corresponding Author

pkral@uic.edu

Notes

The authors declare no competing financial interest.

ACKNOWLEDGMENTS

This work was supported by the ACS PRF grant no. 53062-ND6. I.S. would like to acknowledge the support obtained through the Herbert E. Paaren Summer Research Award and the support from the Camille and Henry Dreyfus Foundation through the Senior Scientist Mentor Award to Prof. Cynthia J. Jameson.

REFERENCES

(1) Rupley, J. A.; Careri, G. *Adv. Protein Chem.* **1991**, *41*, 37.
(2) Weik, M.; Lehnert, U.; Zaccai, G. *Biophy. J.* **2005**, *89*, 3639.
(3) Hummer, G.; Rasaiah, J. C.; Noworyta, J. P. *Nature* **2001**, *414*, 188.
(4) Berezhkovskii, A.; Hummer, G. *Phys. Rev. Lett.* **2002**, *89*, 064503.
(5) Holt, J. K.; Park, H. G.; Wang, Y.; Stadermann, M.; Artyukhin, A. B.; Grigoropoulos, C. P.; Noy, A.; Bakajin, O. *Science* **2006**, *312*, 1034.
(6) Maniwa, Y.; Kataura, H.; Abe, M.; Udaka, A.; Suzuki, S.; Achiba, Y.; Kira, H.; Matsuda, K.; Kadowaki, H.; Okabe, Y. *Chem. Phys. Lett.* **2005**, *401*, 534.
(7) Takaiwa, D.; Hatano, I.; Koga, K.; Tanaka, H. *Proc. Natl. Acad. Sci. U.S.A.* **2008**, *105*, 39.
(8) Patra, N.; Wang, B.; Král, P. *Nano Lett.* **2009**, *9*, 3766.
(9) Yuk, J. M.; Park, J.; Ercius, P.; Kim, K.; Hellebusch, D. J.; Crommie, M. F.; Lee, J. Y.; Zettl, A.; Alivisatos, P. *Science* **2012**, *336*, 61.
(10) Koishi, T.; Yasuoka, K.; Willow, S. Y.; Fujikawa, S.; Zeng, X. C. *J. Chem. Theory Comput.* **2013**, *9* (6), 2540.
(11) Iiyama, T.; Nishikawa, K.; Otowa, T.; Kaneko, K. *J. Phys. Chem.* **1995**, *99*, 10075.
(12) Iiyama, T.; Nishikawa, K.; Suzuki, T. *Chem. Phys. Lett.* **1997**, *274*, 152.
(13) Hirunsit, P.; Balbuena, P. B. *J. Phys. Chem.* **2007**, *111*, 1709.
(14) Han, S.; Choi, M. Y.; Kumar, P.; Stanley, H. E. *Nat. Phys.* **2010**, *6*, 685.
(15) Bai, J.; Angell, A.; Zeng, X. C. *Proc. Natl. Acad. Sci. U.S.A.* **2010**, *107*, 5718.
(16) Phillips, J. C.; Braun, R.; Wang, W.; Gumbart, J.; Tajkhorshid, E.; Villa, E.; Chipot, C.; Skeel, R. D.; Kal, L.; Schulten, K. *J. Comput. Chem.* **2005**, *26*, 1781.
(17) Humphrey, W. *J. Mol. Graphics* **1996**, *14*, 33.
(18) MacKerell, A. D.; Bashford, D.; Bellott, M.; Dunbrack, R. L.; Evanseck, J. D.; Field, M. J.; Fischer, S.; Gao, J.; Guo, H.; Ha, S.; Joseph-McCarthy, D.; Kuchnir, L.; Kuczera, K.; Lau, F. T. K.; Mattos, C.; Michnick, S.; Ngo, T.; Nguyen, D. T.; Prodhom, B.; Reiher, W. E.; Roux, B.; Schlenkrich, M.; Smith, J. C.; Stote, R.; Straub, J.; Watanabe, M.; Wirkiewicz-Kuczera, J.; Yin, D.; Karplus, M. *J. Phys. Chem.* **1998**, *102*, 3586.
(19) Servantie, J.; Gaspard, P. *Phys. Rev. Lett.* **2003**, *91*, 185503.
(20) Wang, B.; Král, P. *J. Am. Chem. Soc.* **2006**, *128*, 15984.
(21) Darden, T.; York, D.; Pedersen, L. *J. Chem. Phys.* **1993**, *98*, 10089.
(22) Park, J. H.; Aluru, N. R. *J. Phys. Chem.* **2010**, *114*, 2595.
(23) Alarcón, L. M.; Malaspina, D. C.; Schulz, E. P.; Frechero, M. A.; Appignanesi, G. A. *Chem. Phys.* **2011**, *388*, 47.
(24) Young, C.; Chaeho, P.; Kwang, S.; Kim, J. *Chem. Phys.* **2006**, *124*, 094308.
(25) Xantheas, S. J. *Chem. Phys.* **1994**, *100*, 7523.
(26) Han, M.; Young, L.; Seung, B.; Tarakeshwar, P.; Kwang, S.; Kim, J. *Chem. Phys.* **2005**, *122*, 044309.
(27) Gregory, J.; Clary, D.; Liu, K.; Brown, M.; Saykally, R. *Science* **1997**, *275*, 814.
(28) Baskin, A.; Lo, W. Y.; Král, P. *ACS Nano* **2012**, *6*, 6083.
(29) Hermansson, K.; Alfredsson, M. *J. Chem. Phys.* **1999**, *111*, 1993.
(30) Wu, K.; Wan, R.; Wang, C.; Ren, X.; Fang, H. *Chin. Phys. Lett.* **2010**, *27*, 034501.
(31) Ojamaee, L.; Hermansson, K. *J. Phys. Chem.* **1994**, *98*, 4271.
(32) Yongjae, L.; Martin, D.; Parise, J.; Hriljac, J.; Vogt, T. *Nano Lett.* **2004**, *4*, 619.